

# On-chip gas detection in silicon optical microcavities

Jacob T. Robinson, Long Chen, and Michal Lipson

Department of Electrical and Computer Engineering, Cornell University Ithaca, NY 14853  
[jtr26@cornell.edu](mailto:jtr26@cornell.edu)

**Abstract:** We demonstrate a chip-scale photonic system for the room-temperature detection of gas composition and pressure using a slotted silicon microring resonator. We measure shifts in the resonance wavelength due to the presence and pressure of acetylene gas and resolve differences in the refractive index as small as  $10^{-4}$  in the near-IR. The observed sensitivity of this device (enhanced due to the slot-waveguide geometry) agrees with the expected value of 490 nm/refractive index unit.

©2008 Optical Society of America

**OCIS codes:** (280.4788) Optical sensing and sensors; (230.5750) Resonators; (130.6010) Sensors.

---

## References and links

1. W. Yang, D. B. Conkey, B. Wu, D. Yin, A. R. Hawkins, and H. Schmidt, "Atomic spectroscopy on a chip," *Nat. Photon* **1**, 331 (2007).
2. C. A. Barrios, K. B. Gylfason, B. Sánchez, A. Griol, H. Sohlström, M. Holgado, and R. Casquel, "Slot-waveguide biochemical sensor," *Opt. Lett.* **32**, 3080 (2007).
3. L. De Stefano, L. Moretti, I. Rendina, and A. M. Rossi, "Porous silicon microcavities for optical hydrocarbons detection," *Sens. Actuators A* **104**, 179 (2003).
4. B. Schmidt, V. Almeida, C. Manolatou, S. Preble, and M. Lipson, "Nanocavity in a silicon waveguide for ultrasensitive nanoparticle detection," *App. Phys. Lett.* **85**, 4854 (2004).
5. A. M. Armani, R. P. Kulkarni, S. E. Fraser, R. C. Flagan, and K. J. Vahala, "Label-free, single-molecule detection with optical microcavities," *Science* **317**, 783 (2007).
6. D. Englund, A. Faraon, I. Fushman, N. Stoltz, P. Petroff, and J. Vuckovic, "Controlling cavity reflectivity with a single quantum dot," *Nature* **450**, 857 (2007).
7. T. Yoshie, A. Scherer, J. Hendrickson, G. Khitrova, H. M. Gibbs, G. Rupper, C. Ell, O. B. Shchekin, and D. G. Deppe, "Vacuum rabi splitting with a single quantum dot in a photonic crystal nanocavity," *Nature* **432**, 200 (2004).
8. J. T. Robinson, C. Manolatou, L. Chen, and M. Lipson, "Ultrasmall mode volumes in dielectric optical microcavities," *Phys. Rev. Lett.* **95**, 143901 (2005).
9. F. Dell'Olio and V.M. Passaro, "Optical sensing by optimized silicon slot waveguides," *Opt. Express* **15**, 4977 (2007) <http://www.opticsexpress.org/abstract.cfm?URI=oe-15-8-4977>.
10. V. R. Almeida, X. Qianfan, C. A. Barrios, and M. Lipson, "Guiding and confining light in void nanostructure," *Opt. Lett.* **29**, 1209 (2004).
11. V. R. Almeida, R. R. Panepucci, and M. Lipson, "Nanotaper for compact mode conversion," *Opt. Lett.* **28**, 1302 (2003).
12. W. C. Gardiner, Jr., "Refractivity of combustion gases," *Combust. Flame* **40**, 213 (1981).
13. K. Nakagawa, M. de Labachellerie, Y. Awaji, and M. Kourogi, "Accurate optical frequency atlas of the 1.5- $\mu$ m bands of acetylene," *J. Opt. Soc. Am. B* **13**, 2708 (1996).
14. P. Dubé, L.-S. Ma, J. Ye, P. Jungner, and J. L. Hall, "Thermally induced self-locking of an optical cavity by overtone absorption in acetylene gas," *J. Opt. Soc. Am. B* **13**, 2041 (1996).
15. R. W. Boyd, *Nonlinear optics* 2nd ed (Academic, San Diego CA, 2003).
16. M. Borselli, T. Johnson, and O. Painter, "Beyond the rayleigh scattering limit in high-q silicon microdisks: Theory and experiment," *Opt. Express* **13**, 1515 (2005) <http://www.opticsexpress.org/abstract.cfm?URI=oe-13-5-1515>.
17. B.-S. Song, S. Noda, T. Asano, and Y. Akahane, "Ultra-high-q photonic double-heterostructure nanocavity," *Nat. Mater.* **4**, 207 (2005).

## 1. Introduction

Interaction of light with matter in a gaseous state is an important functionality for sensors as well as for addressing isolated atomic or molecular states for quantum optic applications [1]. The vast majority of room-temperature experiments involving light-matter interactions in integrated photonic devices have been performed with matter in the solid or liquid state [2-7]. This is primarily due to the typically small refractive index and absorption differences between gasses at optical frequencies. Recently on-chip optical interaction with Rb vapor in ARROW waveguides was demonstrated by exploiting the enhanced optical interaction at atomic resonances [1]. In the absence of such atomic resonances, on-chip room-temperature optical interaction with gasses has remained unexplored, due to the relatively weak strength of interaction.

In order to achieve on-chip optical interrogation of weakly interacting gasses we use a high confinement resonant cavity formed by slotted waveguides. Resonant cavities have proven to be extremely useful as sensors of change in refractive index [2-7], and the slot waveguide geometry allows us to enhance the light-matter interaction with the gas [2, 8, 9]. Therefore, by combining the enhanced light-matter interaction of the slot waveguide with the refractive index sensitivity of the microring resonator we demonstrate here the ability to detect small changes in the refractive index of surrounding gasses.

## 2. Experimental setup

A scanning electron micrograph (SEM) of the 20  $\mu\text{m}$ -diameter silicon microring like the one used for gas detection is shown in Fig. 1(a). The resonant wavelength of the devices is determined by the optical path length in the ring which depends on the effective index of the slot waveguide which, in turn, is determined by the refractive index of the gas surrounding the waveguide. Therefore by measuring changes in the resonant wavelength of the microring ( $\Delta\lambda$ ) we can detect small changes in refractive index of the gas ( $\Delta n_{\text{gas}}$ ) [2]. For changes in  $\Delta n_{\text{gas}}$  small compared to the core-cladding index difference, we can assume that the mode shape does not change. This is equivalent to taking the first-order correction to the resonant wavelength which can be expressed mathematically as:

$$\Delta\lambda = \lambda_0 \left( \Gamma / n_{\text{eff}} \right) \Delta n_{\text{gas}}, \quad (1)$$

where  $\lambda_0$  is the unperturbed resonance wavelength,  $n_{\text{eff}}$  is the unperturbed value of the effective index in the ring, and  $\Gamma$  is the proportionality constant satisfying the relationship  $\Delta n_{\text{eff}} = \Gamma \Delta n_{\text{gas}}$ . We define this proportionality constant as the interaction factor of the guided mode:

$$\Gamma \equiv \frac{n_{\text{gas}} \int_{\text{gas}} |\mathbf{E}|^2 dA}{Z_0 \int_{\infty} (\mathbf{E} \times \mathbf{H}^*) \cdot \hat{\mathbf{z}} dA}, \quad (2)$$

where  $Z_0$  is the impedance of free space,  $\hat{\mathbf{z}}$  is the propagation direction, and the integrals are evaluated over the cross-sectional area of the waveguide. Note that we have defined this interaction factor based on the sensitivity of the waveguide to changes in the cladding index similarly to [9], and this is not equivalent to the power confined to the slot region. This is because in high index contrast structures (unlike weakly confined waveguides such as fibers) the relationship between E and H is no longer linear. Since the polarizability of matter (and thus its refractive index) is determined by the material response to the electric field, it is the concentration of the electric field in the sensing region which is important not the concentration of power.

Using a slot waveguide geometry we enhance the sensitivity of the resonance wavelength to changes in refractive index [9]. By virtue of the boundary conditions at dielectric interfaces,

slot waveguides have been shown to greatly increase the electric field in the low-index slot region for the quasi-TE mode [10]. This has the effect of both increasing  $\Gamma$  according to (2) as well as lowering  $n_{eff}$  which increases the sensitivity according to (1). Figure 1(b) shows a cross-sectional SEM of a slot waveguide like the one used in our device. Based on this geometry we use a finite difference mode solver to calculate the fundamental quasi-TE mode and plot the major electric field component in Fig. 1(c). The sidewall angles and waveguide dimensions of approximately 600 nm wide by 250 nm tall waveguide with a 40 nm slot (measured at the mid-point) are based on the cross sectional SEM in Fig. 1(b). From the results of the mode solver we calculate  $\Gamma$  and  $n_{eff}$  to be 0.64 and 2.01 respectively. Note that this large interaction factor means that the effective index of the slot waveguide changes by 0.64 times the change in index of the gas. This is a surprising result considering that only about 23% of the mode power resides in the gas region. This large interaction factor is the result of the enhanced electric field in the region between the two silicon ridges as shown in Fig. 1(c). According to this ratio of  $\Gamma/n_{eff}$  we expect the slot waveguide to improve the sensitivity of the ring by a more than a factor of 20 compared to a waveguide with the same cross section without a slot. The sensitivity of the device is determined by the factor relating the shift in the resonant wavelength to the shift in refractive index ( $\lambda_0 \Gamma/n_{eff}$ ) which for our device is approximately 490 nm/refractive index unit (RIU). Due to the large index contrast and thus large interaction factor for our device, this quantity is more than a factor of two larger than previously reported slot-based resonant sensors for fluids [2].

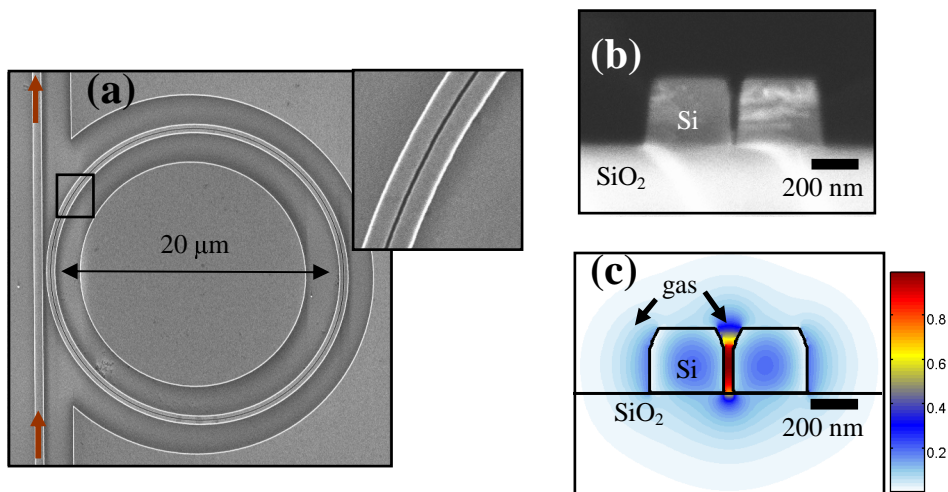


Fig. 1. (a) SEM image of a silicon slotted microring resonator like the one used in our experiment. Inset shows the slot waveguide in the ring. Red arrows show direction of light propagation along the bus waveguide (b) cross sectional SEM image of a slot waveguide like the one in (a). (c) calculated mode profile for the major E-field component of the fundamental quasi-TE mode for the waveguide shown in (b). The high concentration of electric field in the gas region makes the resonator more sensitive to changes in refractive index of the gas.

To control the gas environment surrounding the ring resonator we affix a 1 x 1.5cm glass cell atop the silicon chip using a UV-curable epoxy. We attach flexible tubing connected to hose barbs on either end of the glass cell to control the type and pressure of the gas above the microring resonator. A photograph of the gas cell attached to a silicon chip is shown in Fig.

2(a). A schematic of the experimental setup is shown in Fig. 2(b). Our optical source is a fiber-coupled 5 mW tunable near-IR laser (1520-1620 nm) which is passed through an inline polarization controller (PC) which is adjusted to excite the quasi-TE mode. Using a cleaved fiber and an inverse nanotaper [11] we couple light into the waveguide at the chip edge. To distinguish guided from unguided light we offset the waveguide output by approximately one centimeter as depicted in Fig. 2(a) and (b). The light from the waveguide output at the chip edge is collimated with a collection lens and passed through a polarization filter oriented to pass light polarized in the plane of the chip. The light which passes through the polarizer is measured with an InGaAs photodetector and power meter. By adjusting the PC to maximize the power through the polarization filter we can selectively excite and measure the quasi-TE mode. We record the transmission spectrum by scanning the wavelength of the tunable laser and plotting the collected power as a function of wavelength. Using needle valves we can control the flow of acetylene or compressed air over the chip. A pressure gauge at the output allows us to monitor the gas pressure in the system.

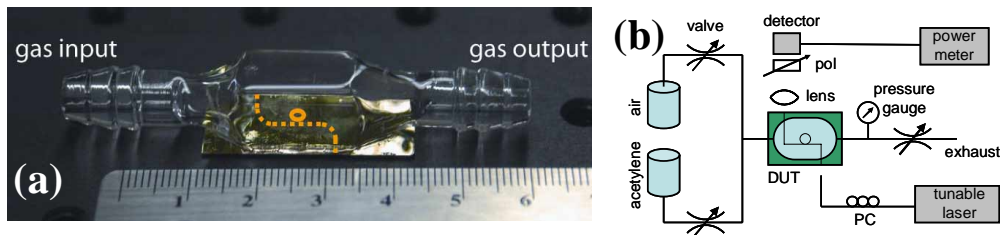


Fig. 2. (a): Photograph of the gas cell affixed to the silicon photonic chip. Dotted line shows the path of the light through the waveguide and the circle denotes the approximate location of the microring. (b) schematic of the experimental setup which was used to measure the resonant wavelength of the microring under different gaseous environments.

### 3. Measurement and analysis

We determine the relative change in refractive index of gasses at various pressures by measuring changes in the resonant wavelength of the microring cavity. Figure 3(a) shows the transmission spectrum for the microring resonator in air (solid) and acetylene gas (dashed) at room temperature and atmospheric pressure. A resonance shift of approximately 0.2 nm is clearly visible. To confirm that the shift in resonance is due entirely to the difference in gasses we repeated the measurement 3 times alternating between air and acetylene. We calculate an average resonance shift of 0.19 nm with a standard deviation of 0.07 nm verifying that the shift in resonance is a reproducible consequence of the changing index of the surrounding gas. At room temperature and atmospheric pressure the difference in index between acetylene and air is approximately  $3.24 \times 10^{-4}$  RIU [12]. According to (1) this index difference should result in a resonance shift of 0.16 nm which agrees with the experimental data within one standard deviation. In Fig. 3(b) we plot the resonance wavelength as a function of acetylene gas pressure. For each pressure, we take three measurements over the course of approximately five minutes. We then fit the measured transmission data to a Lorentzian using a least squares method. Each symbol in Fig. 3(b) represents the average resonant wavelength from the three measurements as determined by the fit. The error bars represent plus and minus one standard deviation. Solid symbols represent the measured resonance shift as the cell is pressurized and open symbols represent measurements as the cell is depressurized. The overlap of these measurements verifies that the shift in resonance wavelength is a reproducible result of the pressure of the surrounding acetylene gas.

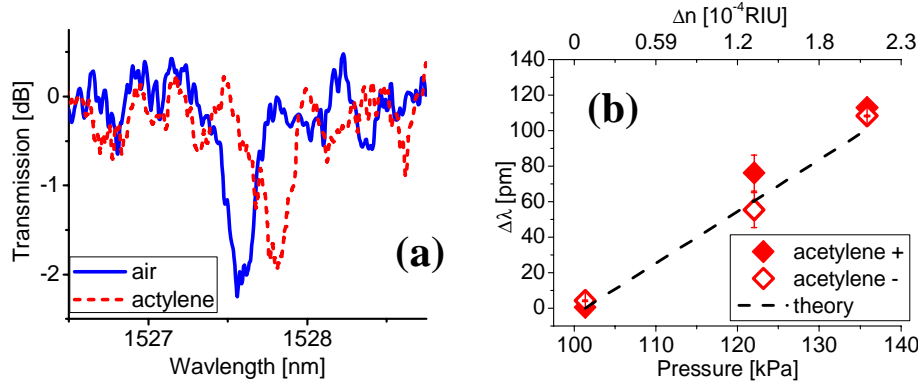


Fig. 3. (a) Transmission spectra for the microring resonator in the presence of air (solid) and acetylene gas (dotted) at room temperature and atmospheric pressure. The shift in resonance is due to the difference in refractive index between air and acetylene gas. (b): Change in resonant wavelength as a function of gas pressure for acetylene. Solid and open shapes represent the average of three measurements for increasing and decreasing pressure respectively. Error bars represent the standard deviation of the three measurements for each data point. Dashed line shows the theoretical resonance shift based on the properties of the resonator. The slope of 490nm/RIU determines the sensitivity of the device.

We verify the measured index change due to variation in pressure by comparing it to the Gladstone-Dale model for the refractive index of gasses as a function of density. According to this model we can write the change in index of the gas ( $\Delta n$ ) as a linear function of the change in pressure ( $\Delta P$ ):

$$\Delta n = \frac{K_{GD}}{RT} \Delta P, \quad (3)$$

where  $K_{GD}$  is the Gladstone-Dale constant,  $R$  is the ideal gas constant, and  $T$  is the temperature. According to [12] we compute the Gladstone-Dale constant for acetylene at a wavelength of 1527.5 nm to be  $K_{GD} = 14.26 \text{ cm}^3/\text{mol}$ . Note that despite the weak molecular resonances which absorb in this wavelength range [13], to a good approximation  $K_{GD}$  can be considered to be constant. This is due to the fact that the overall refractive index of acetylene gas at 20° C and atmospheric pressure is  $n = 1 + 5.93 \times 10^{-4}$  [12] which is due mostly to electronic transitions in the ultra-violet [14]. From the Kramers-Kronig relation we determine the maximum correction to the refractive index from the measured maximum absorption near 1527 nm ( $0.33 \text{ cm}^{-1}$ ) to be approximately  $2 \times 10^{-6}$  [15]. Since this correction is two orders of magnitude smaller than the background index we can neglect this effect and treat  $K_{GD}$  as a constant in this wavelength range. Using the room temperature of 20° C and the calculated values of  $K_{GD}$  and  $\Gamma/n_{eff}$  we combine (3) and (1) to plot the expected shift in resonance wavelength as the dashed line in Fig. 3. This theoretical resonance shift agrees with the measured data within the experimental error. To demonstrate the sensitivity of this device we can rewrite the x-axis in Fig. 3 in terms of the change in refractive index of the gas according to (3). This is plotted as the top x-axis in Fig. 3 showing that our device is sensitive to refractive index changes on the order of  $10^{-4}$ . Note that the slope of the data in Fig. 3 is proportional to the ratio of  $\Gamma/n_{eff}$ . Therefore the sensitivity of this measurement is proportional to the interaction factor and thus more than 20 times greater than the same device without a slot. One should note that the shift in resonant wavelength is dependent only on the ratio  $\Gamma/n_{eff}$  and independent of the cavity quality factor ( $Q = \lambda_0/\Delta\lambda$ , where  $\Delta\lambda$  is the full width half maximum of the resonance). The ability to accurately quantify very small changes in the resonance wavelength will be aided by an increase in  $Q$  since this results in a

narrowing of the resonance linewidth ( $\Delta\lambda$ ). Due to the large value of  $\Gamma/n_{\text{eff}}$  we were able to perform this experiment using a resonator with a relatively modest  $Q$  factor of about 5000. Much larger  $Q$  factors on the order of  $10^6$  and greater have been reported in similar structures by several groups [5, 16, 17] and could greatly improve this technique by allowing more accurate readout of the wavelength shift.

#### 4. Conclusions

Using a silicon slotted microring resonant cavity we have demonstrated a chip-scale photonic system capable of detecting small changes in the refractive index of a gas due to composition and pressure. Due to the nanoscale slot geometry of our resonant cavity we have shown a large interaction factor of 0.64 indicating that the change in effective index of the slot waveguide is 64% of the change in index of the gas despite the fact that only 23% of the mode power resides in the gas region. This large interaction factor leads to a large device sensitivity of 490 nm/RIU. With this device we have demonstrated the detection of refractive index changes on the order of  $10^{-4}$  using a resonator with a  $Q$  factor of 5000. Increasing this  $Q$  factor could further increase the accuracy of this detection scheme.

This platform for the interaction of gas-phase molecules with optical microcavities could open the door for a number of experiments in atomic and molecular optics as well as applications in gas sensing.

#### Acknowledgments

The authors gratefully acknowledge Alexander Gaeta, Pablo Londero, and Aaron Slepko for their helpful discussions. We also thank David Wise for the fabrication of the glass cells and Christina Manolatu for the use of her finite difference mode solver. Research support is gratefully acknowledged from the National Science Foundation Center on Materials and Devices for Information Technology Research (CMDITR), DMR-0120967, the Cornell Center for Material Research, the National Science Foundation's CAREER Grant No. 0446571, and the U.S. Air Force MURI program on "Electrically-Pumped Silicon-Based Lasers for Chip-Scale Nanophotonic Systems" supervised by Dr. Gernot Pomrenke. This work was performed in part at the Cornell NanoScale Facility, a member of the National Nanotechnology Infrastructure Network, which is supported by the National Science Foundation (Grant ECS 03-35765).